Phantom-based evaluation of a semi-automatic segmentation algorithm for cerebral vascular structures in 3D ultrasound angiography (3D USA)

C. Chalopin¹, K. Krissian², A. Müns³, F. Arlt³, J. Meixensberger³, D. Lindner³

¹ Universität Leipzig, ICCAS, Leipzig, Germany
² Universidad de Las Palmas de Gran Canaria, GIMET, Las Palmas, Spain
³ Universität Leipzig, Klinik für Neurochirurgie, Leipzig, Germany

```
Kontakt: claire.chalopin@iccas.de
```

Abstract:

Intraoperative ultrasound angiography (USA) provides to the neurosurgeon real-time information about the cerebral vascular network but is difficult to interpret due to the presence of noise and artifacts. A segmentation algorithm may improve the visualization of data by extracting the vascular structures only. We propose to adapt and test an existing model-based segmentation method on 3D USA data of a vascular phantom with 4 mm tube radii. The performance of the algorithm is evaluated by comparison with a gold standard (CT data) and with manual delineations. The algorithm generated a segmentation model whose radii values are overestimated of more than half of one mm in comparison with the gold standard but with more realistic geometrical features than the manual delineations.

Keywords: 3D ultrasound angiography, vascular segmentation, physical phantom

1   Problem

Intraoperative ultrasound angiography (iUSA) is an imaging modality which, in neurosurgery, enables the surgeon to visualize the real-time information of the anatomy and function of the cerebral vascular network during the intervention [1]. With the development of new ultrasound contrast agents, contrast harmonic imaging (CHI) is becoming an emerging modality, which enables enhancing the main cerebral vascular structures in the images. However, the interpretation of iUSA data may be complex. The image quality is reduced by the speckle, but also by the presence of blood and cerebrospinal liquids which occur during the surgical intervention. The contrast agent induces artifacts as well, called bubble noise and blooming effect. Boundaries of the vascular structures are therefore unclearly defined in the USA data. The extraction of the vascular structures would improve their visualization by keeping the object of interest only and by eliminating noise and artifacts.

Segmentation of vascular structures has already been extensively studied and validated with success on patient data but mainly focuses on good quality images [2]. Some methods have been however adapted on US data. In 3D power Doppler data thresholding techniques ([3]) or region growing algorithms ([4]) are the most common methods used. In 3D B-mode volumes model-based techniques are required to overcome the problem of unclear borders. Two dimensional active contours performing slice by slice ([5]) and a dynamic balloon represented by a triangular mesh ([6]) have been used to segment the carotid contours. Furthermore, Krissian et al [6] proposed a model-based multiscale scheme that computes a vesselness measure to segment the aorta artery. The model is represented by a circular cross-section cylinder. The technique aims estimating the centerline position and radii values of elongated structures in the data. A multiscale implementation allows extracting vascular structures of different sizes. It is then possible to generate a segmentation model from the estimated centerlines and radii values. None of these methods have been validated so far on 3D USA data of the brain.

In this work we aim to quantitatively estimate on a physical vascular phantom the performance of an adapted version of the semi-automatic segmentation method proposed in [6].

2 Methods

Semi-automatic segmentation method

The segmentation method is based on a model-based multiscale detection of the vessel centerlines using a cylindrical model with circular cross-section. Briefly, a vesselness measure is computed for each voxel of the USA volume which represents the probability that a voxel belongs to the centerline of an elongated structure. The vesselness measure at a voxel position is computed based on the image gradient information along a circle C which centre is the voxel itself. Its orientation is defined based on the computation of the eigenvectors of the structure tensor which represent the directions of axis and cross-section of the elongated structure. The structure tensor is computed for a sigma value σ proportional to the radius value r of the elongated structure, representing the radius value of the circle C. Thus, a multi-scale implementation consisting in computing the vesselness measures for N_{scales} different radii values $r_{lower} \leq r \leq r_{upper}$ is used to extract vascular structures of various sizes. For each voxel, the maximum vesselness response is kept in the multiscale space and the corresponding r_{max} value represents an estimation of the radius. In the original method, the user manually selects the vascular structure centerlines in the volume of maximum vesselness responses. In order to reduce the interaction, the maximum vesselness responses are here thresholded with a value $T_{maxvess}$ provided by the user. The centerline segments whose sizes are shorter than a given pruning size $S_{pruning}$ are considered as noise and are automatically eliminated. A surface reconstruction of the vascular structures, called here segmentation model, is then generated based on the extracted centerlines and estimated radii information. The surface is obtained in two steps: i) creation of a volume data representing the distance transform to the estimated tubular structures processing each segment as a circular cylinder, ii) iso-surface generation based on the marching cubes algorithm (Figure 2a).

Physical vascular phantom and 3D US acquisition

The physical phantom includes two silicon tubes mimicking blood vessels whose inside diameter is 4 mm and wall thickness is 1 mm (Figure 1a). The silicon tubes have been laid down into a plastic container filled with gelatine. The acquisition system of the 3D USA data includes a common US device (Sonoline Elegra, Siemens) with a 2D free-hand 2.5 MHz phased array probe, an optical tracking system (NDI, Polaris) and a navigation system (SonoNavigator, Localite). The optical tracking system aims at estimating the position of the US probe in the room. The navigation system is used to compound the set of 2D US images acquired with the US probe within an US volume. The vascular phantom is linked to a pump which simulates a laminar blood flow within the tubes, filled with water. Short before the acquisition, an US contrast agent (SonoVue, Bracco) is injected into the phantom tubes. The operator scans then the phantom surface with the US probe positioned perpendicular to the tube lengths and moved parallel to the tubes. A set of 2D enhanced images is obtained and sent to the navigation system through a S-video connection. A 3D USA volume of voxel size $1 \times 1 \times 1$ mm^3 is eventually reconstructed (Figure 1 b and c).
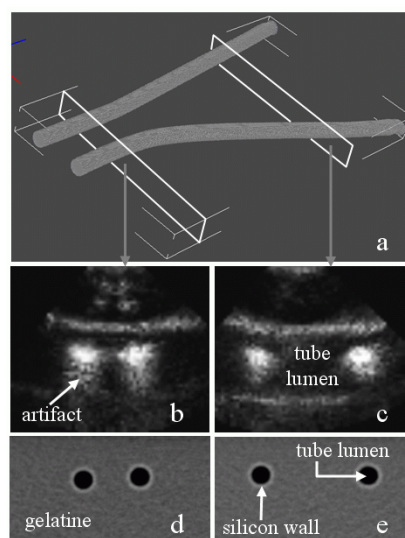

Figure 1: The physical vascular phantom includes two silicon tubes mimicking the blood vessels (a). (b) and (c) are two slices of the 3D USA data acquired with an US contrast agent. (d) and (e) are two slices of the CT volume.

Evaluation of the segmentation algorithm by comparison with a gold standard

We assume that the phantom tube geometrical features may deform during the building (weight of the gelatine) and through the image acquisition process (pressure of the US probe on the phantom surface). We estimate therefore the performance of the segmentation algorithm operating on the 3D USA data by comparison with CT data of the phantom, considered as gold standard. A CT scanner (Philips) is used here in helical mode with 0.33 mm spacing between the slices. The pixel size in the slices is 0.20x0.20 mm². The phantom tubes are filled with water and the scanning performed without the pump for easier practical reasons (Figure 1 d and e).

The extraction of tube lumens in the CT data is performed by a region growing algorithm with upper threshold value set to zero representing the interface between the silicon wall and the water (Figure 2b). Evaluation of the segmentation algorithm performance is done by comparing the tube lumen radii values. As it was already described above, the model-based segmentation algorithm provides an estimate of the radii values for each point of the extracted centerlines. The radii values in the CT data are computed as following. We assume, based on visual observation, that the tube lumens are perpendicular to volume cross-sections, and that therefore the lumen cross-sections are disks. The number of voxels included in the lumen cross-sections is counted in each volume cross-section. It represents the surface S_{CT} and the radii values r_{CT} are then deduced.

Comparison of the segmentation algorithm and manual delineations

Result of the segmentation algorithm is then compared to manual delineations. Seven observers manually delineated the tube lumen borders in the 3D USA data of the phantom using the free ITK-SNAP segmentation tool. The observers needed between 15 to 30 minutes to perform the task. High differences between the manual delineations are observed and the delineation of two observers has been removed due to a too large overestimation of the tube lumens. An average volume has been then computed from the manual delineations of the five remaining observers (Figure 2c).

The geometrical features defined for the comparison are the tube lumen cross-section area and the centerline distance, since the lumen contours in the average delineation are rather elliptic. The cross-section areas are computed for each volume cross-section as the number of lumen voxels. The average delineation has been thinned to extract the lumen centerline and the distance to the centerline of the segmentation model computed for each volume cross-section.
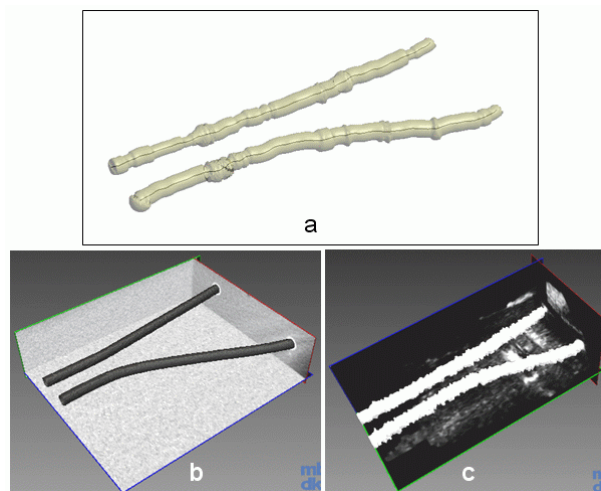

Figure 2: Phantom tube lumens extracted by (a) the segmentation algorithm in the 3D USA data, (b) a region growing method in the CT data and (c) manual delineations performed in the 3D USA data by observers and averaged.

3   Results

Segmentation model generation

The tube lumens have been segmented in the 3D USA data using the segmentation method previously described. Although the known dimensions of the silicon tubes in the phantom are constant, the tube lumen diameters do not look homogeneous in the 3D USA data. The segmentation algorithm has been therefore applied in a multi-scale manner with

the following values: r_{lower}=0.5, r_{upper}=5.0 and N_{scales}=10. Thus, a large set of radii values are tested by the algorithm. The segmentation model has been generated with $T_{maxvess}$=15.0 and $S_{pruning}$=5 (Figure 2a).

<u>Comparison of the segmentation model with the gold standard and the average delineation</u>
Geometrical features have been calculated on the segmentation model, the gold standard and the average delineation as previously explained. Since the voxel size is different in both volumes, the mean values and standard deviations have been used for the comparison (Table 1). Values show that the mean radii values in the segmentation model are larger than nearly one millimeter in comparison to the real tube lumen size and larger than more than half of a millimeter in comparison to the gold standard. The mean cross-section areas estimated by the observers are twice larger than those values in the gold standard although this report is smaller than two in the comparison between the segmentation model and the gold standard. The mean centerline distance values calculated between the segmentation model and the mean delineation is less than one voxel (0.8 ± 0.6 mm for tube 1 and 0.6 ± 0.6 mm for tube 2). The tube centerlines are therefore estimated nearly at the same position by the algorithm and the observers.

	radii values (mm)		cross-section area (mm^2)	
	tube 1	tube 2	tube 1	tube 2
phantom	2.0	2.0	12.6	12.6
gold standard	2.24 ± 0.04	2.30 ± 0.05	15.8 ± 0.6	16.5 ± 0.7
average delineation	-	-	41.6 ± 6.8	38.6 ± 5.2
segmentation model	2.80 ± 0.43	3.03 ± 0.38	30.0 ± 5.8	25.9 ± 7.2

Table 1: Comparison of the segmentation model with the gold standard and the average delineation using the radii and cross-section area features.

4   Discussion

Comparison results showed that the mean radius value of the segmentation model generated by the algorithm is overestimated of more than half of a millimeter in comparison with the gold standard. Two main reasons may explain this difference. First, the image resolution in the US data is lower, increasing the partial volume effect. The tube lumen diameters look visually larger than 4 voxels. Second, the tube lumen cross-sections in the US data look rather like an ellipse, due to the US probe pressure during the data acquisition. Visually, the circular cross-sections of the segmentation model have for radii values the largest ellipse axis. Moreover the geometrical features calculated in the gold standard are slightly larger than the real tube sizes meaning that the phantom deformed. We showed moreover that the observers still more overestimated the tube lumen cross-section area than the segmentation algorithm did it. They have been more hindered by noise and artifacts in the data to correctly delineate the unclear tube borders. We conclude that the segmentation algorithm succeeded therefore, on our vascular phantom, in providing a model with realistic geometrical features regarding the low image resolution of the 3D USA data and in eliminating noise and artifacts. Moreover, processing time for the multi-scale scheme was less than one minute for a volume of 62x71x145 voxels. The algorithm parameters r_{lower}, r_{upper}, N_{scales} and $S_{pruning}$ may be set fixed, also for patient data. Only the threshold value $T_{maxvess}$ for extracting the vascular structures has to be tuned since its value is a compromise between the among of information and the among of noise in the segmentation model. However, the segmentation tool is suitable for the operating room.
Next step will consist in evaluating the segmentation algorithm on a more realistic vascular phantom including tubes of different radii values and close to the cerebral vascular anatomy and with bifurcations. It should be interesting to check the behavior of the segmentation algorithm on thinner tubes and bifurcations. Tests on intraoperative 3D USA data of patients is planed as well since the goal of the project is to integrate the segmentation model of the intraoperative cerebral vascular network into a navigation system. Applications might be the guidance of the neurosurgeon to reach the tumor without damaging the surrounding blood vessels or the check of the success of aneurysm clipping surgeries.

5   References

[1]   Unsgaard G, Rygh OM, Selbekk T, Müller TB, Kolstad F, Lindseth F, Nagelhus Hernes TA. Intra-operative 3D ultrasound in neurosurgery. Acta Neurochir 2006;148:235-253.
[2]   Kirbas C, Quek Francis. A review of vessel extraction techniques and algorithms. ACM Computing Surveys 2004;36(2):81-121.

[3]   Reinertsen I, Lindseth F, Unsgaard G, Collins DL. Clinical validation of vessel-based registration for correction of brain-shift. Medical Image Analysis 2007;11:673-684.

[4]   Hold S, Hensel K, Winter S, Dekomien C, Schmitz G. Segmentation of blood vessels in 3D ultrasound-datasets by a model-based region growing algorithm In Proceedings of Computer Assisted Orthopaedic Surgery (CAOS) 2007:610-603.

[5]   Gill J, Ladak H, Steinman D, Fenster A. Accuracy and Variability Assessment of Semi-Automatic Technique for Segmentation of the Carotid Arteries from 3D Ultrasound Images. Medical Physics 2000;27(6):1333-1342.

[6]   A Zahalka, A Fenster. An automated segmentation method for three-dimensional carotid ultrasound images. Phys Med Biol 2001;46:1321-1342.

[7]   Krissian K, Ellsmere J, Vosburgh K, Kikinis R, Westin CF. Multiscale segmentation of the aorta in 3D ultrasound images. Proceedings of the 25th Annual Int. Conf. on the IEEE Engineering in Medicine and Biology Society, EMBS, Cancun Mexico 2003:638-641.